

An efficient numerical simulation of the cyclic loading experiments on RC structures

Georgios Ch. Lykidis^a and Konstantinos V. Spiliopoulos*

*Institute of Structural Analysis and Antiseismic Research, National Technical University of Athens,
Department of Civil Engineering, Zografou Campus, Zografou 157-73, Athens, Greece*

(Received May2, 2012, Revised October1, 2013, Accepted November 16, 2013)

Abstract. In this work a numerical method to simulate the response of reinforced concrete structures subject to cyclically imposed displacements is proposed. The method consists of a combination of a displacement and load controlled version of the Newton–Raphson iterative technique, used for the loading and the unloading part of the cycles respectively. The whole procedure is combined with a relatively simple concrete model whose only material parameter is its uniaxial compressive strength. The proposed methodology may realistically simulate, in an easy way, the physical process of any experimentally tested RC structure under imposed displacements cycles. The efficiency of the approach is demonstrated through a series of analyses of experimentally tested specimens reported in the literature.

Keywords: reinforced concrete, nonlinear analysis, cyclic loading, smeared crack model, 3D solid finite element

1. Introduction

During the last decades, the numerical prediction of the response of Reinforced Concrete (RC) structures has been a very popular field of research. Most related published work has been based on the finite element method of analysis (ACI 1997) using either elements of two/three dimensional elasticity or of a more macroscopic nature (e.g. fiber or simple beam elements). Although the former ones have considerable computational cost restrictions, they have been extensively used for the analysis of simple structures or individual structural members (such as beams, columns, shear walls or joints). The choice of these elements is argued by the fact that they can give far more realistic results especially when they predict modes of nonlinearity other than that of flexure, for example brittle shear failures.

Most numerical applications are restricted to RC members under monotonic loading, mainly due to the complexities involved in the modelling of the material under any arbitrary cyclic loading history. When it comes to applications with cyclic loads, most of them have been performed with two dimensional elements and only a few use three dimensional solid elements. A brief literature review of the pertinent work presented to date is given next.

*Corresponding author, Associate Professor., E-mail: kvspilio@central.ntua.gr

^aPh.D., E-mail: lykidis@gmail.com

Darwin and Pecknold (1977) use a procedure with 2D four-node isoparametric quadrilateral finite elements for simulating the response of cyclically loaded planar RC structures. The analytical predictions show reasonable agreement with experimental findings. Rule and Rowlands (1992) developed a biaxial constitutive model which they used together with triangular plane elements to analyze a deep orthogonally reinforced beam. The results exhibit a good approximation compared to experimental data. Ozbolt and Bazant (1992) implemented their microplane model into quadrilateral plane stress finite elements after extending it to include cyclic loading. They demonstrate applications on plain concrete specimens loaded in bending and compression without any sign reversals. Inoue *et al.* (1997) proposed a nonlinear finite element model for the dynamic analysis of a 3D RC shear wall subjected to earthquake motions. An 8-node plane quadrilateral element is used to model a test specimen of the wall with H-shaped section. Comparison with experimental results shows good accuracy. Balan *et al.* (1997) presented a 3D concrete material model for finite element analysis and comparisons with experimental data are performed on the material level concluding to quite realistic predictions. Vecchio (1999) presented a finite element model that provides analysis capability for arbitrary loading conditions, including reversed cyclic loads. He used 2D plane finite elements to analyze a shear wall and three large scale panel elements. The resulting analysis procedure exhibited adequate convergence and stability characteristics. Ile and Reynouard (2000) propose a constitutive model for predicting the cyclic response of RC structures which adopts the concept of a smeared crack approach assuming a plane stress condition. Predictions of the model compare quite well with experimental data on shear walls under monotonic and cyclic loading and also on a shear wall structure which was tested under a large number of cyclic load reversals due to earthquake loading. All analyses use 2D plane elements. Balan *et al.* (2001) presented a hypoplastic model for three dimensional analysis under arbitrary loads. Correlation studies with available experimental tests at the material level confirm a good model performance. Kwan and Billington (2001) perform an evaluation of finite element modelling approaches for predicting cyclic behavior of structural concrete. They also use 8-node isoparametric plane elements. Kwon and Spacone (2002) use the model, developed by Balan *et al.* (2001), for the analysis of concrete specimens and RC columns subjected to different load patterns. Concrete was modelled with 8-node brick elements and only the monotonic loading envelope was followed in the numerical simulations. Further 2D plane analyses can be found in Palermo and Vecchio (2002) and Kwak and Kim (2004). In the framework of 2D applications, Au and Bai (2007) added a bond-slip behaviour modelled by contact elements. He *et al.* (2008) employed a more complicated fracture energy based concrete model. A similar model was used by Sasmal *et al.* (2010) to analyze beam-column joints under plane stress conditions. Recently, To *et al.* (2009) incorporated a strut-and-tie model into a conventional planar frame model. Sharma *et al.* (2010) managed to approximate the strength degradation of RC beam-column joints by performing a nonlinear pushover analysis. The use of fiber elements for the cyclic analysis of RC beams was demonstrated, quite recently, by Melo *et al.* (2011) in a review article. Some applications with 3D solid elements and cyclic loading have been performed by Girard and Bastien (2002), Ozbolt and Li (2001), Spiliopoulos and Lykidis (2006), Lykidis and Spiliopoulos (2008).

The purpose of the present work is to discuss the numerical simulation of cyclic loading experiments on RC structures. Experimental data on members under cyclic actions are usually presented with load – displacement curves. In many cases there is a gradual degradation of the capacity of these members with increasing number of cycles. For this reason a displacement controlled method of analysis seems more appropriate for the simulation of such experiments.

Nevertheless it can be proven that, for both 2D plane and 3D solid elements, if a plain

displacement control iterative method of nonlinear analysis is directly employed throughout the whole range of loading cycles, unrealistic cracking may lead to unexpected sudden divergence. Therefore the application of displacement controlled algorithms is not so straight forward. To the authors' knowledge, this deficiency has not been observed by any of the researchers that have performed RC nonlinear analyses.

In this work, in order to obtain a realistic prediction for such cyclic loading cases, a combination of load and displacement controlled iterative procedures, is proposed. It is proved that this approach may simulate any cyclic loading experiment under displacement control in a most natural way. After a brief description of the employed material and finite element modelling in Section 2, the theoretical description of the plain load controlled and displacement controlled procedures are presented in Section 3 together with their numerical implementations. The suggested methodology with the combination of the two procedures is described in Section 4 and numerical applications are presented in Section 5. The technique proves to be stable and can provide convergence for RC structures under cyclic load reversals even if extended nonlinearities are exhibited.

2. Brief review of the material and finite element modeling

The concrete modelling of Kotsovos and Pavlovic (1995), the development of which was based on extensive experimental investigation, is used in this work. According to this model, the constitutive behaviour is treated in the three-dimensional space with two distinct parts of nonlinearity which depend on the stress state. For low stresses microcracking causes small amount of nonlinearity, whereas for larger stresses macrocracking causes brittle loss of material continuity. Any effect of material strain softening both in tension or compression is therefore ignored.

The stress state is described with reference to the octahedral stress which may be decomposed into a hydrostatic σ_0 and a deviatoric part τ_0 . The simplicity of the model lies in the fact that these stress components are expressed as functions of the uniaxial compressive concrete strength f_c only.

It is an experimental fact that the component of the non-linear deformation is much larger under τ_0 rather than under σ_0 and therefore it is τ_0 that determines whether a crack forms. When a stress state reaches the locus of the ultimate deviatoric stresses that defines concrete's failure surface, a crack forms in the direction perpendicular to the maximum principal tensile stress.

The highly non-linear problem is analyzed using incremental steps with iterations. Using the material stress state of the last iteration one may evaluate the predicted stress level σ_{pr} at the current one. The evaluation of the predicted stress at a Gauss point (GP) highly depends on whether cracks have already appeared in previous iterations.

If there was no crack, then a check is made on whether a new crack is currently opening. In case the crack criterion is fulfilled, then two actions are taken:

- a) A crack forms at a plane perpendicular to the direction of the maximum principal tensile stress. This stress is zeroed resulting to the development of a residual stress vector $\Delta\sigma_r$.
- b) The material properties of the corresponding concrete element are changed so that no stiffness is retained along the axis perpendicular to the plane of the crack. For numerical reasons a

small amount of shear stiffness is kept along the plane by multiplying the shear modulus with an appropriate shear retention factor.

If there is still no crack opening at this GP, the GP is checked whether it is in a state of further loading or un-loading. Different actions are taken with respect to what state (loading or un-loading) this GP was in the previous iteration. These actions result to different updates of the material properties as well as to residual stresses $\Delta\sigma_r$.

In case there are crack(s) at a GP at the previous iteration, it is checked whether the total strains perpendicular to the crack plane/planes have now become compressive. Then the crack(s) are assumed to close and the material properties that were altered to accommodate the crack(s) are recovered. A vector of residual stresses $\Delta\sigma_r$ is also formed.

Three cracks at different directions are allowed to form at a GP before it loses its load carrying capacity.

Uniaxial truss elements are used to model reinforcement which is considered embedded in the concrete element by using the appropriate embedded truss bar formulations of Barzegar and Maddipudi (1997). The Menegotto–Pinto model that accounts for the Bauschinger effect is used as a constitutive law for reinforcing steel.

The numerical models are developed with twenty seven–node Langrangian brick elements with 3x3x3 GPs. Mesh in objectivity inherent to all brittle materials is alleviated by keeping the size of the elements in the range of 5–20 cm. It is argued that this corresponds to an equivalent volume for each GP approximately of the same size of the concrete specimens that were used in the experiments to derive the concrete behavior (Kotsovos and Pavlovic 1995).

The above procedures have been implemented as an additional module in the finite element code FE77. A more detailed description of the above material and finite element modelling procedures may be found in Spiliopoulos and Lykidis (2006).

3. Numerical approaches used for the nonlinear analysis of RC structures

The Newton – Raphson iterative procedure, commonly used to solve nonlinear systems of equations in finite element analyses, may have two alternative forms: (a) with control of the applied load and (b) with control of the applied displacement. Following a brief review of the basic features of these two methods, their numerical implementations, in conjunction with the concrete material behaviour that was described above, are developed.

3.1 Analysis with load control

The following system of non–linear equilibrium equations has to be solved

$$\mathbf{f}_s(\mathbf{u}) = \mathbf{R} \quad (1)$$

where \mathbf{f}_s is the internal force vector, \mathbf{u} the displacement vector and \mathbf{R} the external force vector, (bold letters denote vectors and matrices).

The solution may be accomplished through incremental load steps according to the standard Newton – Raphson iterative procedure. Linearizing around the displacements of the last converged incremental load step, denoted by i , a prediction for the current step $i+1$ is derived:

$$\mathbf{f}_{s,i+1} = \mathbf{f}_{s,i}(\mathbf{u}) + \left. \frac{\partial \mathbf{f}_s}{\partial \mathbf{u}} \right|_{\mathbf{u}_i} \cdot \Delta \mathbf{u}^{(1)} \quad (2)$$

Since Eq. (1) should be satisfied at the ends of the previous, as well as of the current step, a first estimate of the increments of the displacements may be found from Eq. (3)

$$\mathbf{K}^{(0)} \cdot \Delta \mathbf{u}^{(1)} = \mathbf{R}_{i+1} - \mathbf{R}_i \quad (3)$$

where $\mathbf{K} = \frac{\partial \mathbf{f}_s}{\partial \mathbf{u}}$ is the tangent stiffness matrix of the whole structure.

The updated displacements $\mathbf{u}_{i+1}^{(1)} = \mathbf{u}_i + \Delta \mathbf{u}^{(1)}$ lead to strains and then to stresses, which when integrated, result in a first estimate of the internal force vector $\mathbf{f}_{s,i}^{(1)}$.

A linearizing around this update of the displacements results in

$$\mathbf{f}_{s,i+1} = \mathbf{f}_{s,i}(\mathbf{u}_{i+1}^{(1)}) + \left. \frac{\partial \mathbf{f}_s}{\partial \mathbf{u}} \right|_{\mathbf{u}_{i+1}^{(1)}} \cdot \Delta \mathbf{u}^{(2)} = \mathbf{f}_{s,1}^{(1)} + \mathbf{K}^{(1)} \cdot \Delta \mathbf{u}^{(2)} \quad (4)$$

Once again the left hand side of (4) should be \mathbf{R}_{i+1} and from this equation the next update of the displacements at the end of the current step is derived.

The steps of the numerical procedure inside an incremental step, using the nonlinear material behaviour described in Section 2, may now be developed

1. Initialize data: $\mathbf{u}^{(0)} = \mathbf{u}_i$, $\Delta \mathbf{R}^{(0)} = \mathbf{R}_{i+1} - \mathbf{R}_i$
2. Calculations for each iteration $j = 1, 2, 3, \dots$:
 - 2.1 Compute $\mathbf{K}^{(j-1)}$
 - 2.2 Solve $\mathbf{K}^{(j-1)} \cdot \Delta \mathbf{u}^{(j)} = \Delta \mathbf{R}^{(j-1)} \Rightarrow \Delta \mathbf{u}^{(j)} = \dots$
 - 2.3 $\mathbf{u}^{(j)} = \mathbf{u}^{(j-1)} + \Delta \mathbf{u}^{(j)}$
 - 2.4 $\boldsymbol{\varepsilon}^{(j)} = \boldsymbol{\varepsilon}^{(j-1)} + \Delta \boldsymbol{\varepsilon}^{(j)}$
 - 2.5 $\boldsymbol{\sigma}_{pr}^{(j)} = \boldsymbol{\sigma}^{(j-1)} + \mathbf{D}^{(j-1)} \cdot \Delta \boldsymbol{\varepsilon}^{(j)}$
 - 2.6 Compute residual stresses $\Delta \boldsymbol{\sigma}_r$ and current stresses $\boldsymbol{\sigma}^{(j)} = \boldsymbol{\sigma}_{pr}^{(j)} + \Delta \boldsymbol{\sigma}_r$ as suggested in Section 2 and in Spiliopoulos & Lykidis (2006).
 - 2.7 Compute internal forces $\mathbf{f}_s^{(j)} = \int \mathbf{B}^T \boldsymbol{\sigma}^{(j)} dV$.
 - 2.8 $\Delta \mathbf{R}^{(j)} = \mathbf{R}_{i+1} - \mathbf{f}_s^{(j)}$
3. Replace j by $j+1$ and repeat steps 2.1 – 2.8 if convergence is not achieved.

In all the expressions above, \mathbf{D} is the material matrix for either a concrete or a steel element. This matrix is updated according to the state of cracked, un-cracked, loading or unloading. \mathbf{B} denotes the corresponding compatibility matrix used also to form, by integration in the standard way, the stiffness matrix of the structure assuming full bond between steel and concrete

(Spiliopoulos and Lykidis 2006). A different formulation that assumes partial bond between concrete and reinforcement through the use of bond – slip modelling may be found in Lykidis and Spiliopoulos (2008).

3.2 Analysis with displacement control

In this case the nodal displacements are partitioned into two groups: \mathbf{u}_1 are the free displacements and \mathbf{u}_2 are the prescribed ones

$$\mathbf{u} = \{\mathbf{u}_1, \mathbf{u}_2\}^T \quad (5)$$

At the same time the internal force vector may be also partitioned into $\mathbf{f}_s = \{\mathbf{f}_{s1}, \mathbf{f}_{s2}\}^T$. The non-linear equations of equilibrium may then be written as

$$\mathbf{f}_{s1}(\mathbf{u}_1, \mathbf{u}_2) = \mathbf{0} \quad (6)$$

$$\mathbf{f}_{s2}(\mathbf{u}_1, \mathbf{u}_2) = \mathbf{F} \quad (7)$$

As seen above, in this work zero applied loading at the free displacement group shall be considered. \mathbf{F} denotes the reactions at the points where the displacements are prescribed.

For a given set of prescribed displacements \mathbf{u}_2 Eq.(6) may be solved iteratively to provide the displacements \mathbf{u}_1 , which, together with \mathbf{u}_2 , are substituted in Eq. (7) to get the reaction forces (Jirasek and Bazant 2002).

To solve (6), one may linearize around the displacements of the last incremental prescribed displacement's step i , making a prediction for the current one $i+1$

$$\mathbf{f}_{s1,i+1} = \mathbf{f}_{s1,i}(\mathbf{u}_{1,i}, \mathbf{u}_{2,i}) + \left. \frac{\partial \mathbf{f}_{s1}}{\partial \mathbf{u}_1} \right|_{\mathbf{u}_{1,i}} \cdot \Delta \mathbf{u}_1^{(1)} + \left. \frac{\partial \mathbf{f}_{s1}}{\partial \mathbf{u}_2} \right|_{\mathbf{u}_{2,i}} \cdot \Delta \mathbf{u}_2^{(1)} \quad (8)$$

and since the internal forces of the previous time step as well as the sought internal forces at the end of the current one should be zero

$$\mathbf{K}_{11}^{(0)} \cdot \Delta \mathbf{u}_1^{(1)} + \mathbf{K}_{12}^{(0)} \cdot \Delta \mathbf{u}_2^{(1)} = \mathbf{0} \quad (9)$$

where $\Delta \mathbf{u}_2^{(1)} = \mathbf{u}_{2,i+1} - \mathbf{u}_{2,i}$ is the known increment of the prescribed displacements.

The following notion has also been used

$$\mathbf{K}_{11} = \frac{\partial \mathbf{f}_{s1}}{\partial \mathbf{u}_1}, \mathbf{K}_{12} = \frac{\partial \mathbf{f}_{s1}}{\partial \mathbf{u}_2} \quad (10)$$

where the current tangent stiffness matrix \mathbf{K} has been partitioned as:

$$\mathbf{K} = \begin{bmatrix} \mathbf{K}_{11} & \mathbf{K}_{12} \\ \mathbf{K}_{21} & \mathbf{K}_{22} \end{bmatrix} \quad (11)$$

The increment of the displacements $\Delta \mathbf{u}_1^{(1)}$ may be calculated from (9) and an update of the displacements at the end of the incremental step is derived

$$\mathbf{u}_{1,i+1}^{(1)} = \mathbf{u}_{1,i} + \Delta \mathbf{u}_1^{(1)} \quad (12)$$

This may lead to strains and then to stresses, which when integrated, results in a first estimate of the internal force vector $\mathbf{f}_{s,i}^{(1)}$.

The linearization around $\mathbf{u}_{1,i+1}^{(1)}$, just found, gives

$$\begin{aligned} \mathbf{f}_{s1,i+1} &= \mathbf{f}_{s1,i}(\mathbf{u}_{1,i+1}^{(1)}, \mathbf{u}_{2,i+1}^{(1)}) + \left. \frac{\partial \mathbf{f}_{s1}}{\partial \mathbf{u}_1} \right|_{\mathbf{u}_{1,i+1}^{(1)}} \cdot \Delta \mathbf{u}_1^{(2)} + \left. \frac{\partial \mathbf{f}_{s1}}{\partial \mathbf{u}_2} \right|_{\mathbf{u}_{2,i+1}^{(1)}} \cdot \Delta \mathbf{u}_2^{(2)} = \mathbf{f}_{s1,i}^{(1)} + \left. \frac{\partial \mathbf{f}_{s1}}{\partial \mathbf{u}_1} \right|_{\mathbf{u}_{1,i+1}^{(1)}} \cdot \Delta \mathbf{u}_1^{(2)} \\ &= \mathbf{f}_{s1,i}^{(1)} + \mathbf{K}_{11}^{(1)} \cdot \Delta \mathbf{u}_1^{(2)} \end{aligned} \quad (13)$$

since there are no further increments of $\Delta \mathbf{u}_2$.

Once again the l.h.s. of (13) should be zero. Therefore a new update for $\mathbf{u}_{1,i+1}^{(2)} = \mathbf{u}_{1,i+1}^{(1)} + \Delta \mathbf{u}_1^{(2)}$ may be calculated.

One may now develop the steps of the numerical procedure inside an incremental step:

1. Initialize data

$$\mathbf{u}_1^{(0)} = \mathbf{u}_{1,i}, \Delta \mathbf{u}_2^{(1)} = \mathbf{u}_{2,i+1} - \mathbf{u}_{2,i}, \mathbf{f}_{s1}^{(0)} = \mathbf{0}$$

2. Calculations for each iteration $j = 1, 2, 3, \dots$

$$2.1 \quad \Delta \mathbf{u}_2^{(j)} = \mathbf{0}, \text{ for } j = 1, 2, 3, \dots$$

2.2 Compute $\mathbf{K}^{(j-1)}$ and partition

$$2.3 \quad \text{Solve } \mathbf{K}_{11}^{(j-1)} \cdot \Delta \mathbf{u}_1^{(j)} = -\mathbf{f}_{s1}^{(j-1)} - \mathbf{K}_{12}^{(j-1)} \cdot \Delta \mathbf{u}_2^{(j)} \Rightarrow \Delta \mathbf{u}_1^{(j)} \dots$$

$$2.4 \quad \mathbf{u}_1^{(j)} = \mathbf{u}_1^{(j-1)} + \Delta \mathbf{u}_1^{(j)}$$

$$2.5 \quad \boldsymbol{\varepsilon}^{(j)} = \boldsymbol{\varepsilon}^{(j-1)} + \Delta \boldsymbol{\varepsilon}^{(j)}$$

$$2.6 \quad \boldsymbol{\sigma}_{pr}^{(j)} = \boldsymbol{\sigma}^{(j-1)} + \mathbf{D}^{(j-1)} \cdot \Delta \boldsymbol{\varepsilon}^{(j)}$$

2.7 Compute residual stresses $\Delta \boldsymbol{\sigma}_r$ and current stresses $\boldsymbol{\sigma}^{(j)} = \boldsymbol{\sigma}_{pr}^{(j)} + \Delta \boldsymbol{\sigma}_r$, as suggested in section 2 and in Spiliopoulos and Lykidis (2006).

$$2.8 \quad \text{Compute internal forces } \mathbf{f}_s^{(j)} = \int \mathbf{B}^T \boldsymbol{\sigma}^{(j)} dV.$$

3. Replace j by $j+1$ and repeat steps 2.1 – 2.8 if convergence is not achieved.

4. Proposed method for cyclic loading

Many experiments in RC are displacement driven and are controlled by the deflection at the point of application. In the analytical simulation of these tests this point is considered as an additional support with a prescribed displacement and the force applied on the structure is the



Fig. 1 Typical history of prescribed cyclic displacements imposed at the midspan of a simply supported beam

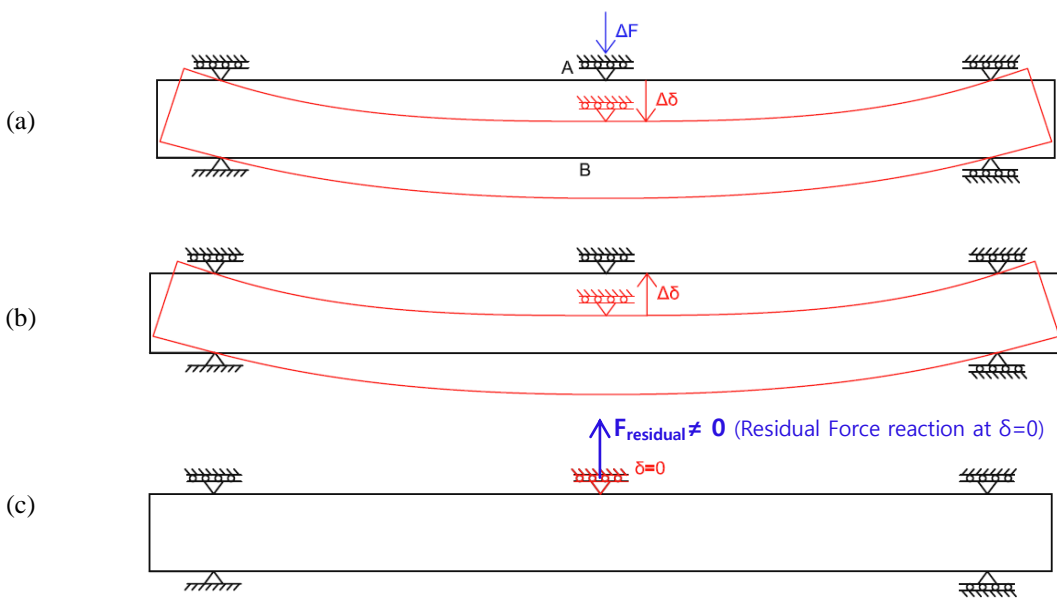


Fig. 2 Schematic representation of a plain displacement controlled approach

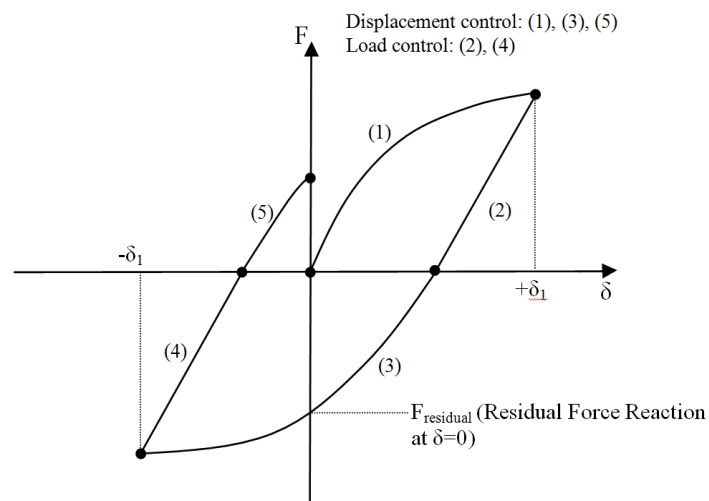


Fig. 3 Typical load – displacement curve

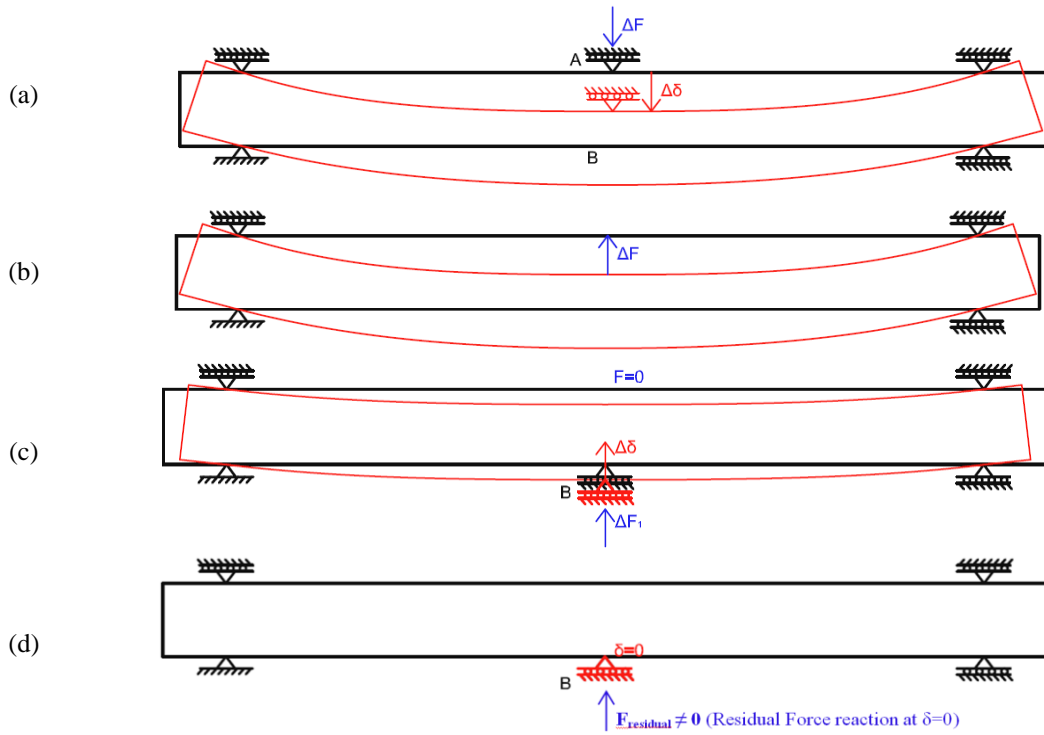


Fig. 4 Schematic representation of the proposed method for half of the cycle

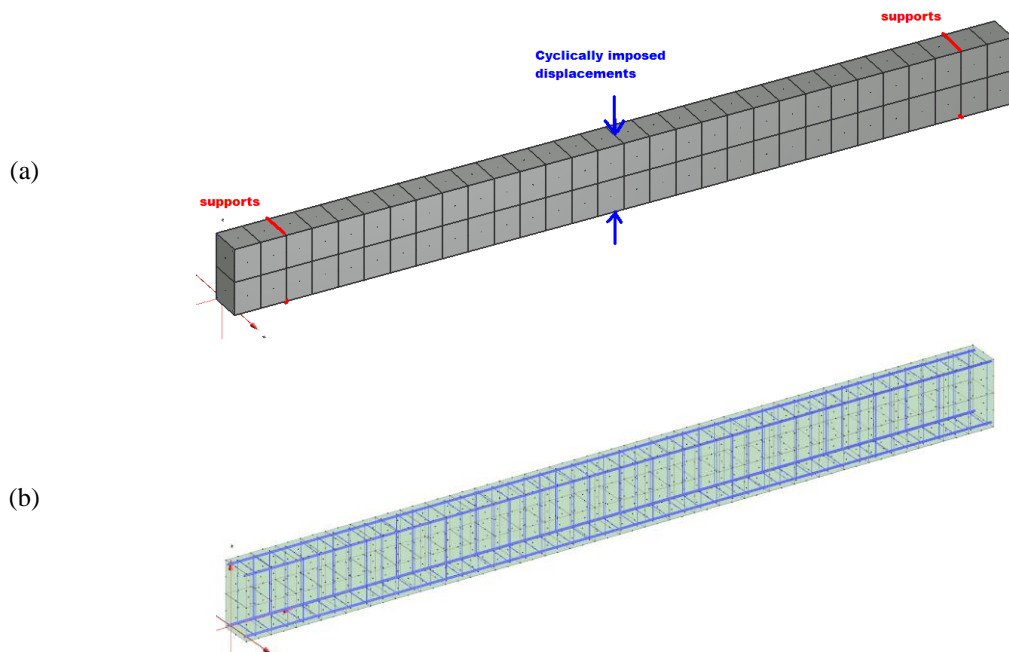


Fig. 5(a) Simply supported beam under cyclically imposed displacements, modeled with hexahedral finite elements (b) Embedded reinforcement element mesh

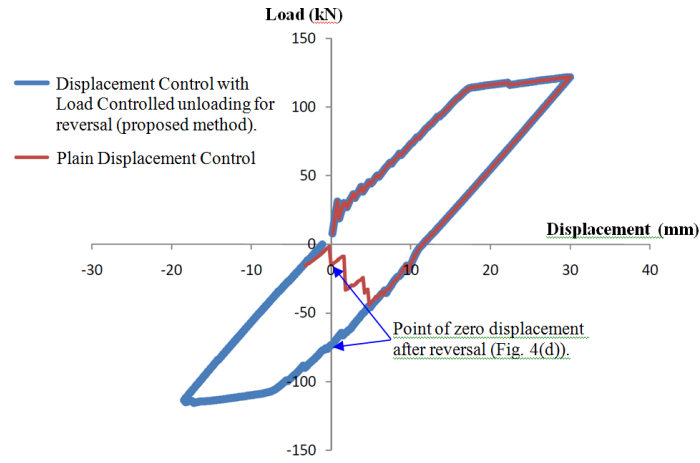


Fig. 6 Load – displacement curves for the analyses of the RC simply supported beam

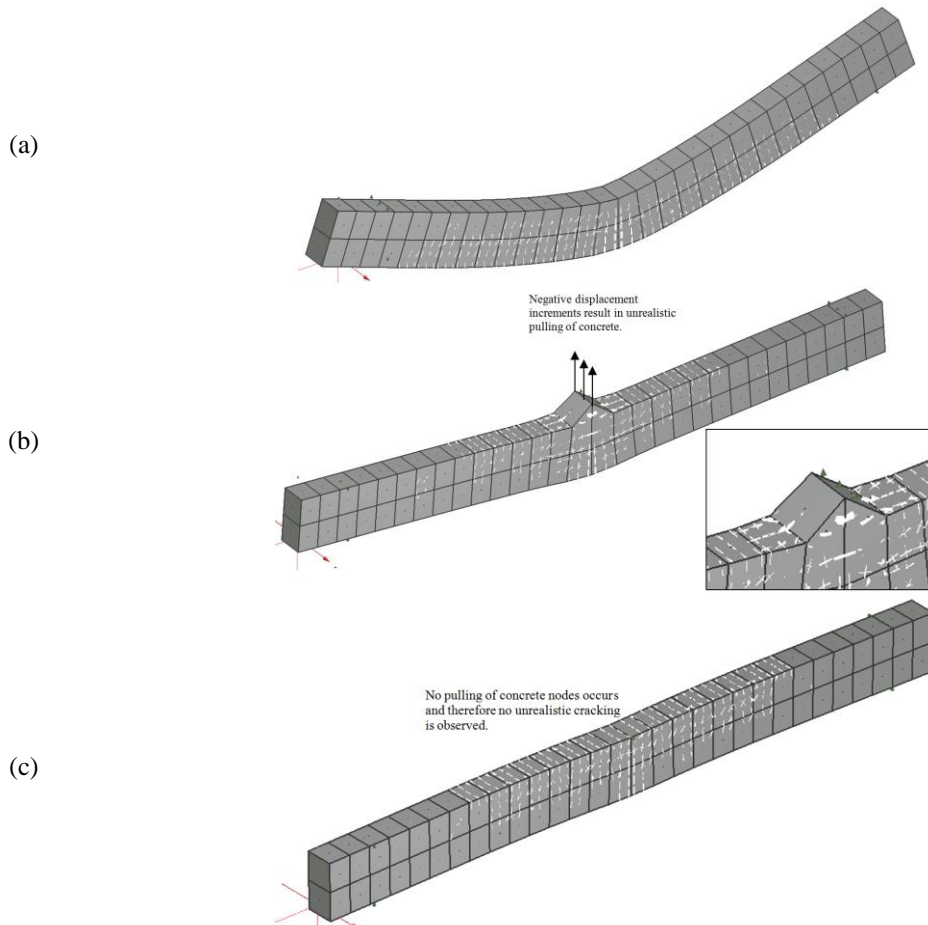


Fig. 7 Predicted cracking at (a) initial stages of loading, (b) after load reversal at point of zero displacement with the plain displacement controlled analysis and (c) after load reversal at point of zero displacement with the analysis according to the proposed methodology.

reaction generated by the support. Under a monotonic loading a plain direct displacement control as the one described above in section 3 may be used to get an estimate of the limit load as well as, possibly, to trace the post-peak range of the load – displacement curve.

The numerical simulation of a cyclic loading, however, is not so straightforward. A combination of displacement controlled/load-controlled procedure needs to be used, which simulates the exact physical procedure of a cyclic loading experiment.

In Fig. 1 (a) one may see the application of a cyclically imposed displacement at the midspan of a simply supported RC beam during an experiment. This loading would produce, at the two displacement peaks, the deformation modes of Fig. 1(b).

A plain displacement control approach would involve the following phases:

- (a) positive applied displacement increments at point A up to a certain displacement (say δ_1) (Fig. 2(a))
- (b) negative applied displacement increments at point A (Fig. 2(b)) down to zero displacement (Fig. 2(c))
- (c) negative applied displacement increments at point B down to displacement $-\delta_1$
- (d) positive applied displacement increments at point B up to displacement zero.

An expected typical load – displacement curve may be seen in Fig. 3.

It may be easily realized that such an approach, during the application of negative displacement increments of phase (b), would result in forces pulling the concrete, a state which is not only highly unrealistic, because such pulling does not occur during an experiment, but also numerically may lead to divergence of the analysis, as will be demonstrated below.

Instead of this approach the following numerical simulation method of such an experiment is proposed in this work (Fig. 4): The specimen is being pushed under displacement control (Fig. 4(a)) up to the displacement δ_1 . This results to the portion marked as (1) in the load–displacement curve of Fig. 3. This force is then recovered (Fig. 4(b)) under force control, resulting to movement along (2) in the force–displacement curve. Then the next stage starts, with a displacement control strategy, marked along (3), which leads to the opposite displacement $-\delta_1$, after passing through the end of the half-cycle ($\delta = 0$) (Fig. 4(c), (d)). Similarly a force controlled approach is followed for the first reloading path denoted as (4) whereas a displacement controlled one completes the cycle along (5). With this procedure the structure is constantly being “pushed” and thus the whole physical process is accurately simulated.

The efficiency of the proposed method is depicted in a set of comparative finite element analyses of a simply supported RC beam subject to an applied displacement history from zero to +30 mm and then to –20 mm (Fig. 5). This application was chosen as the simplest possible case of a cyclically loaded RC member in order to demonstrate how the proposed modelling methodology can avoid exhibiting an unrealistic divergence from a reasonable load – displacement prediction.

The beam has a section of 300 × 600 mm with 2Φ20 mm at the top and bottom and Φ8 mm/150 mm longitudinal and transverse reinforcement respectively. The first analysis is performed with the application of subsequent imposed displacement increments from the top of the beam up to 30 mm and then negative displacement increments up to 0 mm. After that point, new negative displacement increments on the opposite side are applied up to a displacement of -20 mm. The second analysis is performed for the same end displacements of +30 mm/-20 mm but with the use of load controlled unloading for load reversal as proposed in the previous paragraphs. The results of both analyses in terms of load – displacement curves are presented in Fig. 6.

It may be easily noticed that the plain displacement control analysis exhibits a diverging unrealistic behavior exactly after the point of zero load. The negative displacement increments

result to forces pulling the concrete nodes thus leading to unrealistic cracking which makes the solution to diverge. One such stage, the end of half-cycle, for example, with the analytically predicted cracking at midspan may be seen in Fig. 7(b).

On the contrary, the analysis with the proposed methodology, which genuinely simulates the conditions of an experiment, does not exhibit any such unrealistic characteristics (Fig. 7(c)).

It should be noted that the employment of contact elements on both opposite faces of the member could allow a more accurate plain displacement control method which would not exhibit the same unrealistic simulation. Nevertheless this would also impose modelling part of the experimental set up (contact elements would need to be connected at both of their sides), thus making the whole modelling effort more exhaustive. The strategy proposed in this work does not require such additional modelling.

5. Applications

The above described technique was applied in two types of shear walls for which experimental data were available. Applications of cyclic loading on other member types such as beam column joints may also be simulated, with the above procedures, for cases where experimental results exist, e.g. Lykidis and Spiliopoulos (2008) and Tran (2012).

5.1 Shear walls W2 and W4 of Cervenka (1970)

Two identical shear walls, experimentally investigated by Cervenka (1970) under monotonic and cyclic loading, were analyzed first. It should be noted that, in the past, Ile and Reynouard (2000) also analyzed these walls, but in that case, a load controlled procedure was employed.

The shear wall W2, experimentally tested under monotonically increasing applied displacement, was analyzed with the plain direct displacement controlled iterative procedure. The detailing of the shear wall in terms of dimensions and reinforcement can be seen in Fig. 8. Within a zone of 15cm from the bottom, a horizontal reinforcement of 1.84% was provided and in the rest of the specimen the reinforcement percentage was equal to 0.92%. The percentage of the vertical reinforcement was 0.92% along the whole width of the wall. The compressive concrete strength was measured to be $f_c=26.5\text{MPa}$, whereas the steel had a yield limit of $f_{sy}=360\text{MPa}$ and a Young's elastic modulus of 192GPa.

Due to the symmetry of the problem half of the wall was modelled using hexahedral solid elements (Fig. 9). A monotonic displacement was imposed according to the loading history of the experiment and the results of the analysis can be seen in Fig. 10. One can easily see the good matching between the experimental and analytical results, with respect both to stiffness and strength.

The shear wall W4 that was experimentally tested under cyclic loading by the same researcher (Cervenka 1970), was analyzed next. The geometry is the same with the wall W2 but the horizontal and vertical reinforcement is of the order of 1.2%. The displacement history was imposed, under the proposed strategy, and the results appear in Fig. 11. As one can see, analytical results match very well with the behaviour of the specimen both in terms of stiffness, strength and dissipated energy during the large cycle of loading.

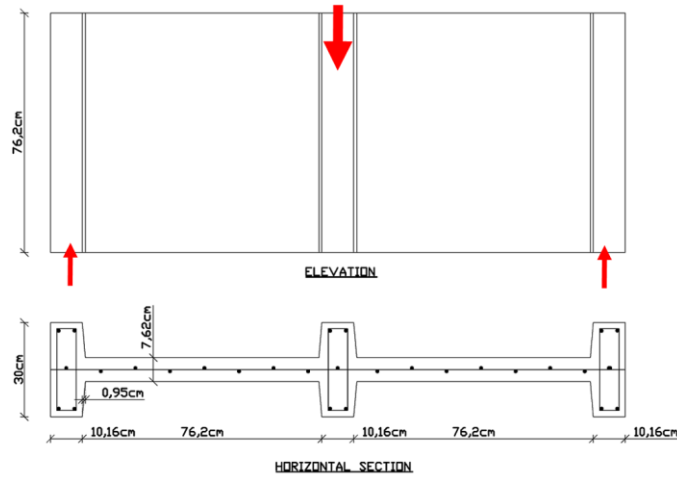


Fig. 8 Dimension and reinforcement detailing of shear wall W2 experimentally tested by Cervenka(1970)

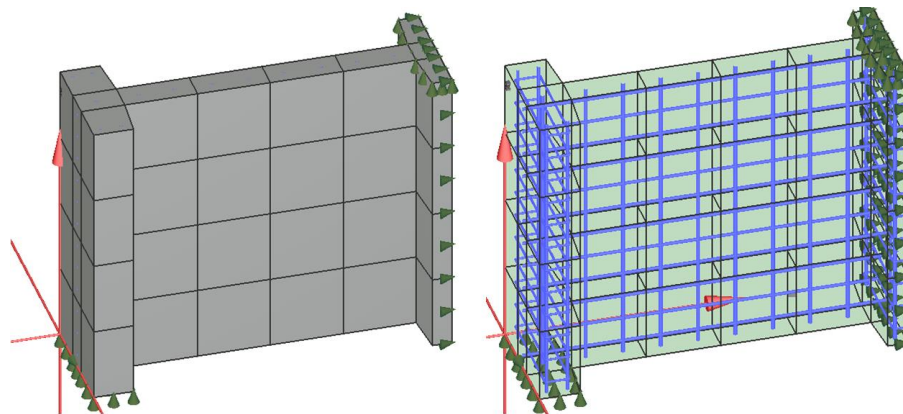
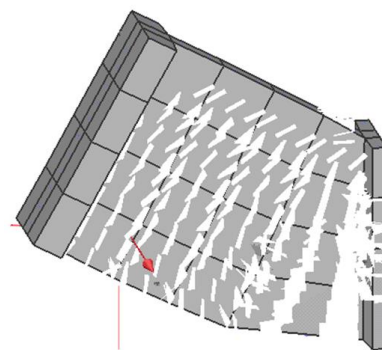
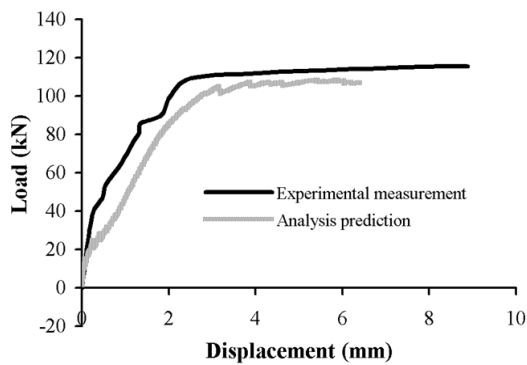


Fig. 9 Finite Element model of shear walls W2 and W4 of Cervenka(1970), concrete elements (left) and embedded reinforcement mesh (right)



(a) Experimental and analytical load – displacement curves (b) crack pattern prediction at the last steps of the analysis

Fig. 10 Shear wall W2, experimentally tested under monotonic loading.

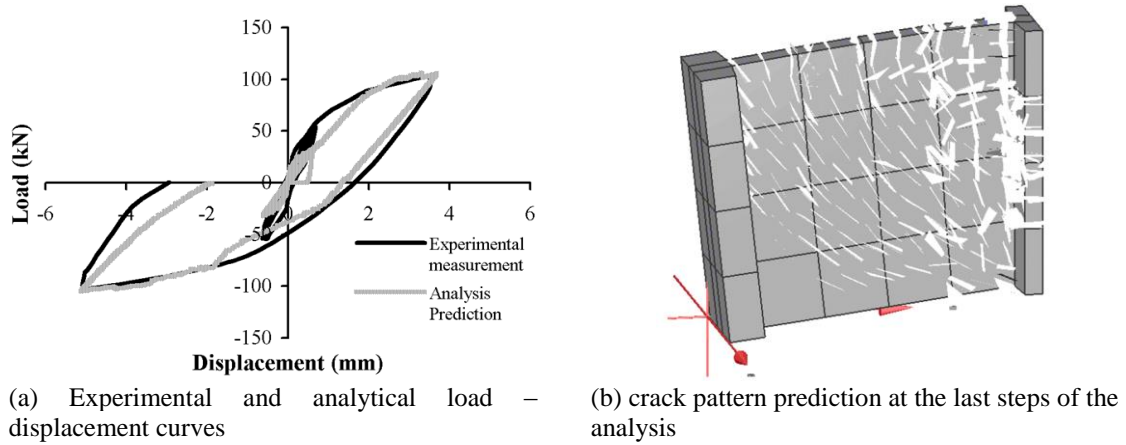


Fig. 11 Shear wall W4 experimentally tested under cyclic loading.

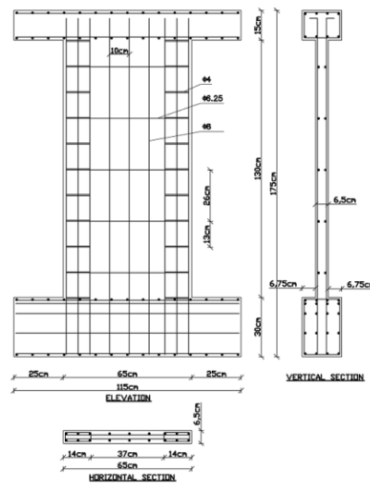


Fig. 12 Dimension and reinforcement detailing of shear wall SW33 experimentally tested by Lefas and Kotsivos (1990)

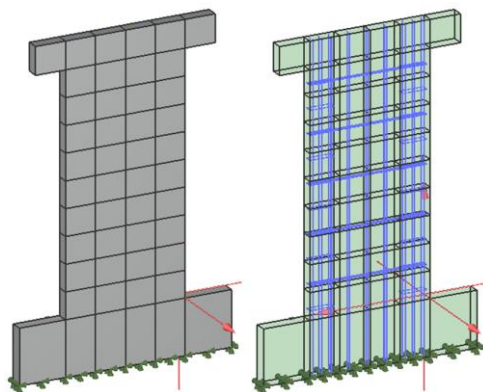


Fig. 13 Finite element model of shear wall SW33 of Lefas and Kotsivos(1990), concrete elements (left) and embedded reinforcement mesh (right).

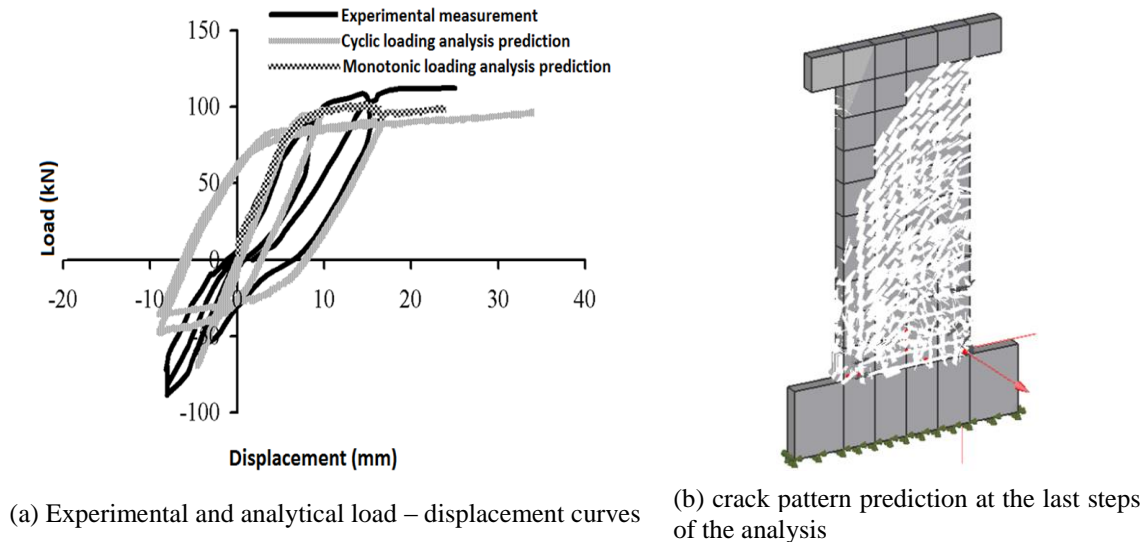


Fig. 14 Shear wall SW33

5.2 Shear wall of lefas and kotsovos (1990)

The shear wall SW33 that was experimentally investigated by Lefas and Kotsovos (1990) was also analyzed using the proposed methodology. The details of reinforcement of the shear wall are depicted in Fig. 12. Rebars of $\Phi 8$ mm, $\Phi 6.25$ mm and $\Phi 4$ mm had a yield and strength limit of $f_{sy} = 470\text{MPa} / f_{su} = 565\text{MPa}$, $f_{sy} = 520\text{MPa} / f_{su} = 610\text{MPa}$, $f_{sy} = 420\text{MPa} / f_{su} = 490\text{MPa}$ respectively. The compressive strength of concrete was 49.20MPa .

Contrary to the previous example, such an experiment may be performed through a monolithically connected rigid block which remains virtually uncracked throughout the duration of the test. In this case, one would include additional FE discretization of the block. However, no extra discretization is needed if one uses the proposed procedure, thus showing its versatility. The specimen was modeled with hexahedral elements according to Fig. 13. A cyclic displacement was imposed on the top beam ends. The results of the analysis and the comparison with experimental data may be seen in Fig. 14.

Although stable hysteresis loops are obtained, for this extreme magnitude of applied displacements there is a weakness of the analysis to give satisfactory predictions. The pinching of the load – displacement curves is significantly underestimated (width of the hysteresis loop appears to be greater than the experimental one) and the specimen's ultimate strength is underestimated with the progress of the cycles. This appears to be due to the fact that after the first cycle at displacements corresponding to the ultimate limit state, extensive cracking (Fig. 14(b)) in the compressive zone of the lower sections near the base indicate significant failure. Consequently, concrete capacity in this area remains very low and therefore the only elements contributing in the behaviour are the reinforcing bars. As the analysis exhibits a stable solution, without the iterative procedure diverging, this inadequacy to provide a more realistic description of concrete under extreme compressive cyclic stresses should be regarded as a weakness of the employed concrete model and not a deficiency of the proposed numerical methodology presented in this paper.

6. Conclusions

In the present work a numerical strategy that deals with the nonlinear analysis of RC structures subjected to cyclic actions is proposed. The strategy is based on a combination of a displacement controlled procedure used for the loading part and a force controlled procedure used for the unloading part of each cycle. For each one of these loading/unloading procedures, the boundary conditions at the points of application are modified appropriately in order to reflect the exact physical conditions of a displacement controlled cyclic loading RC structure experiment. No extra rigid or contact elements are required to simulate the experimental set up.

The proposed numerical strategy is combined with an existing concrete nonlinear material model which has proved to successfully model brittle crack opening and closure under load reversals. The effectiveness of the combined approach is demonstrated with the analysis of two types of shear walls for which experimental data were available.

References

- ACI Committee 446 (1997), *Finite element analysis of fracture in concrete structures: State of the art report*. ACI 446:3E-97, ACI, Detroit.
- Au, F.T.K. and Bai, Z.Z. (2007), "Two-dimensional nonlinear finite element analysis of monotonically and non-reversed cyclically loaded RC beams", *Eng. Struct.*, **29**, 2921-2934.
- Balan, T.A., Filippou, F.C. and Popov, E.P. (1997), "Constitutive model for 3D cyclic analysis of concrete structures", *J. Eng. Mech.- ASCE*, **123**, 143-153.
- Balan, T.A., Spacone, E. and Kwon, M. (2001), "A 3D hypoplastic model for cyclic analysis of concrete structures", *Eng. Struct.*, **23**, 333-342.
- Barzegar, F. and Maddipudi, S. (1997), "Three-dimensional modelling of concrete structures II: Reinforced concrete", *J. Struct. Eng.- ASCE*, **123**(10), 1347-1356.
- Cervenka, V. (1970), *Inelastic finite element analysis of reinforced concrete panels under in-plane loads*, PhD thesis, University of Colorado, Michigan.
- Darwin, D. and Pecknold, D.A. (1977), "Analysis of cyclic loading of plane R/C structures", *Comput. Struct.*, **7**(1), 137-147.
- FE77 v. 2.56, Hinchings D.– User's and Programmer's Manual. Imperial College, London, 2001.
- Girard, C. and Bastien, J. (2002), "Finite Element bond slip model for concrete columns under cyclic loads", *J. Struct. Eng.- ASCE*, **128**, 1502-1510.
- He, W., Wu, Y.F. and Liew, K.M. (2008), "A fracture energy based constitutive model for the analysis of reinforced concrete structures under cyclic loading", *Comput. Meth. Appl. Mech. Eng.*, **197**, 4745-4762.
- Ile, N. and Reynouard, J.M. (2000), "Nonlinear analysis of reinforced concrete shear wall under earthquake loading", *J. Earthq. Eng.*, **4**(2), 183-213.
- Inoue, N., Yang, K. and Shibata, A. (1997), "Dynamic nonlinear analysis of RC shear wall by fem with explicit analytical procedure", *Earthq. Eng. Struct. Dyn.*, **26**, 967-986.
- Jirasek, M. and Bazant Z.P. (2002), *Inelastic Analysis of Structures*, Wiley, West Sussex, England.
- Kotsovos, M.D. and Pavlovic, M.N. (1995), *Structural concrete, finite element analysis for limit state design*, Thomas Telford, London, UK.
- Kwak, H.G. and Kim, D.Y. (2004), "Material nonlinear analysis of RC shear walls subject to cyclic loading", *Eng. Struct.*, **26**, 1423-1436.
- Kwan, W.P. and Billington S.L. (2001), "Simulation of structural concrete under cyclic load", *J. Struct. Eng.- ASCE*, **127**, 1391-1401.
- Kwon, M. and Spacone, E. (2002), "Three-dimensional finite element analyses of reinforced concrete columns", *Comput. Struct.*, **80**, 199-212.
- Lefas, I.D. and Kotsovos, M.D. (1990), "Strength and deformation characteristics of reinforced concrete

- walls under load reversals”, *ACI Struct. J.*, **87**(6), 716-726.
- Lykidis, G.Ch. and Spiliopoulos K.V. (2008), “3D solid finite element analysis of cyclically loaded RC structures allowing embedded reinforcement slippage”, *J. Struct. Eng.-ASCE*, **134**(4), 629-638.
- Melo, J., Fernandes, C., Varum, H., Rodrigues, H., Costa, A. and Arêde, A. (2011), “Numerical modelling of the cyclic behaviour of RC elements built with plain reinforcing bars”, *Eng. Struct.*, **33**, 273-286.
- Ozbolt, J. and Bazant, Z.P. (1992), “Microplane model for cyclic triaxial behavior of concrete”, *J. Eng. Mech. -ASCE*, **118**, 1365-1386.
- Ozbolt, J. and Li, Y.J. (2001), Three dimensional cyclic analysis of compressive diagonal shear failure, Finite Element Analysis of RC Structures, Eds: Willam K, Tanabe T., *ACI-SP-205-4*, 61-79.
- Palermo, D. and Vecchio, F.J. (2002), “Behaviour of 3d RC shear walls”, *ACI Struct. J.*, **99**, 81-89.
- Rule, W.K. and Rowlands, R.E. (1992), “Predicting behaviour of cyclically loaded RC structures”, *J. Struct. Eng. -ASCE*, **118**, 603-616.
- Sasmal S., Novák B. and Ramanjaneyulu K. (2010), “Numerical analysis of under-designed reinforced concrete beam-column joints under cyclic loading”, *Comput. Concr.*, **7**(3), 203-220.
- Sharma, A., Reddy, G.R., Eligehausen, R., Vaze, K.K., Ghosh, A.K. and Kushwaha, H.S. (2010), “Experiments on reinforced concrete beam-column joints under cyclic loads and evaluating their response by nonlinear static pushover analysis”, *Struct. Eng. Mech.*, **35**(1), 99-117.
- Spiliopoulos, K.V. and Lykidis, G.C. (2006), “An efficient three dimensional solid finite element dynamic analysis of reinforced concrete structures”, *Earthq. Eng. Struct. Dyn.*, **35**, 137-157.
- To, N.H.T., Sritharan, S. and Ingham, J.M. (2009), “Strut-and-tie nonlinear cyclic analysis of concrete frames”, *J. Struct. Eng. - ASCE*, **135**(10), 1259-1268.
- Tran, C.T.N. (2012), “Modeling of non-seismically detailed columns subjected to reversed cyclic loadings”, *Struct. Eng. Mech.*, **44**(2), 163-178.
- Vecchio, F.J. (1999), “Towards cyclic load modeling of reinforced concrete”, *ACI Struct. J.*, **96**(2), 193-202.